



**Forchheimer flow to a well considering time-dependent critical radius**

Q. Wang et al.

This discussion paper is/has been under review for the journal Hydrology and Earth System Sciences (HESS). Please refer to the corresponding final paper in HESS if available.

# Forchheimer flow to a well considering time-dependent critical radius

Q. Wang<sup>1</sup>, H. Zhan<sup>1,2</sup>, and Z. Tang<sup>1</sup>

<sup>1</sup>School of Environmental Studies, China University of Geosciences, Wuhan, Hubei, 430074, P. R. China

<sup>2</sup>Department of Geology and Geophysics, Texas A & M University, College Station, TX 77843-3115, USA

Received: 11 October 2013 – Accepted: 3 November 2013 – Published: 19 November 2013

Correspondence to: H. Zhan (zhan@geos.tamu.edu)

Published by Copernicus Publications on behalf of the European Geosciences Union.

[Title Page](#)

[Abstract](#)

[Introduction](#)

[Conclusions](#)

[References](#)

[Tables](#)

[Figures](#)

[⏪](#)

[⏩](#)

[◀](#)

[▶](#)

[Back](#)

[Close](#)

[Full Screen / Esc](#)

[Printer-friendly Version](#)

[Interactive Discussion](#)



## Abstract

Previous studies on the non-Darcian flow into a pumping well assumed that critical radius ( $R_{CD}$ ) was a constant or infinity, where  $R_{CD}$  represents the location of the interface between the non-Darcian flow region and Darcian flow region. In this study, a two-region model considering time-dependent  $R_{CD}$  was established, where the non-Darcian flow was described by the Forchheimer equation. A new iteration method was proposed to estimate  $R_{CD}$  based on the finite-difference method. The results showed that  $R_{CD}$  increased with time until reaching the quasi-steady state flow, and the asymptotic value of  $R_{CD}$  only depended on the critical specific discharge beyond which flow became non-Darcian. A larger inertial force would reduce the change rate of  $R_{CD}$  with time, and resulted in a smaller  $R_{CD}$  at a specific time during the transient flow. The difference between the new solution and previous solutions were obvious in the early pumping stage. The new solution agreed very well with the solution of previous two-region model with a constant  $R_{CD}$  under quasi-steady flow. It agreed with the solution of the fully Darcian flow model in the Darcian flow region, and with the solution of the fully non-Darcian flow model in the non-Darcian flow region near the well.

## 1 Introduction

Darcy's law indicates a linear relationship between the fluid velocity and the hydraulic gradient (Bear, 1972), which is a basic assumption used to handle a great deal of problems related to flow in porous and fractured media. However, many evidences from the laboratory and field experiments show that this linear law may be invalid in some situations, especially when the groundwater flow velocity is sufficiently high or sufficiently low, where non-Darcian flow prevails (Basak, 1977; Bordier and Zimmer, 2000; Englund, 1953; Forchheimer, 1901; Izbash, 1931; Liu et al., 2012; Soni et al., 1978).

## HESD

10, 14095–14129, 2013

### Forchheimer flow to a well considering time-dependent critical radius

Q. Wang et al.

Title Page

Abstract

Introduction

Conclusions

References

Tables

Figures

⏪

⏩

◀

▶

Back

Close

Full Screen / Esc

Printer-friendly Version

Interactive Discussion



## Forchheimer flow to a well considering time-dependent critical radius

Q. Wang et al.

Title Page

Abstract

Introduction

Conclusions

References

Tables

Figures

⏪

⏩

◀

▶

Back

Close

Full Screen / Esc

Printer-friendly Version

Interactive Discussion

and Todman (2010) showed that the Jacob method, based on Darcy's law, cannot fit the step-drawdown tests of van Tonder et al. (2001) when the pumping rate is greater  $10 \text{ m}^3 \text{ h}^{-1}$ . However, the Forchheimer law fitted the step-drawdown tests data very well (Mathias and Todman, 2010). In this study, we will focus on the non-Darcian flow into a pumping well by the Forchheimer law.

Although many efforts have been devoted to study the non-Darcian flow around the well, the exact solutions have not been obtained due to the non-linearity of the problem (Mathias et al., 2008; Yeh and Chang, 2013). For example, Sen (1990, 2000) employed the Boltzmann transform to analytically solve the problems related to the non-Darcian flow. This method was showed to be problematic, since both initial and boundary conditions cannot be simultaneously transformed into a form only containing the Boltzmann variable (Camacho and Vasquez, 1992; Wen et al., 2008a). Wen et al. (2008a, b) obtained the semi-analytical solutions of the non-Darcian flow model by combining the linearization procedure and the Laplace transform method (LL method). This LL method assumed that transient flow in the non-Darcian flow region can be taken as a quasi-steady state flow. Wen et al. (2008a, 2008b) pointed out that solutions by the Boltzmann transform and the LL method coincided at late time. To test the accuracy of the semi-analytical solutions (Wen et al., 2008a; Sen, 2000), Mathias et al. (2008) and Wen et al. (2009) employed the finite-difference method to study the non-Darcian flow problems, and their results showed that the semi-analytical solution only agreed very well with the numerical solution at late pumping stage.

All above-mentioned investigations assume that the non-Darcian flow occurs over the entire domain, which is called a fully non-Darcian flow (F-ND) model hereinafter. In fact, the regime of the flow to the pumping well can be divided into two regions: non-Darcian flow occurs within a narrow region around well, due to the relatively high velocity of flow there, and Darcian flow prevails over the rest domain. One may think that such two-region flow could be described by the Forchheimer law, which would automatically reduce to the Darcy's law at the location far from the well (because the second-order velocity term in the Forchheimer law will be negligible if velocity approaches zero).



## Forchheimer flow to a well considering time-dependent critical radius

Q. Wang et al.

Title Page

Abstract

Introduction

Conclusions

References

Tables

Figures

⏪

⏩

◀

▶

Back

Close

Full Screen / Esc

Printer-friendly Version

Interactive Discussion

post-linear laminar flow, and (D) non-Darcy post-linear turbulent flow (Basak, 1977; Bear, 1972). For radial flow to a pumping well, the velocity in the aquifer decreases with the distance from the well. Therefore, the radial flow might experience all four-flow regimes. To simplify the problem, we use a two-region model that considers a non-Darcian flow region near the well and a Darcian flow region away from the well. A unique feature of the two-region model used in this study is that the critical radius is allowed to vary with time whereas it was assumed to be constant in previous studies (Dudgeon et al., 1972a, b; Huyakorn and Dudgeon, 1976, 1978; Mackie, 1983; Sen, 1988; Wen et al., 2008b).

Generally, the start of the non-Darcian flow can be determined by the critical Reynolds number ( $Re_C$ ), where the Reynolds number is defined as

$$Re(r, t) = D_p q(r, t) / \nu, \quad (1)$$

where  $\nu$  is the kinematic viscosity of the fluid ( $L^2T^{-1}$ );  $D_p$  is the characteristic grain diameter (L);  $q(r, t)$  is specific discharge ( $LT^{-1}$ ) at distance  $r$  (L) and time  $t$  (T);  $Re$  is Reynolds number which depends on time and space (dimensionless). The critical Reynolds number ( $Re_C$ ) refers to  $Re$  at the start of non-Darcian flow. Up to present, there is still considerable debate on  $Re_C$  for the initiation of non-Darcian flow in porous media. Bear (1972) pointed out that  $Re_C$  varied between 3 to 10; Scheidegger (1974) gave  $Re_C$  to be 0.1 to 75; Zeng and Grigg (2006) suggested the range of  $Re_C$  as 1 to 100.  $Re_C$  will be set as 10 in this study. According to Eq. (1), one can see that the specific discharge has a linear relationship with  $Re$ . Therefore, the critical specific discharge ( $q_C$ ) can also be used to determine the start of the non-Darcian flow, since one can calculate  $q_C$  for a given  $Re_C$ . When the specific discharge is less than or equal to  $q_C$  (or  $Re \leq Re_C$ ), the flow is considered as Darcian. When the specific discharge is greater than  $q_C$  (or  $Re > Re_C$ ), the flow is taken as non-Darcian. Denoting  $R_C(t)$  as the critical radius at which  $q = q_C$  (or  $Re = Re_C$ ), then it is non-Darcian flow when  $r \leq R_C(t)$  and Darcian flow when  $r > R_C(t)$ , as shown in Fig. 1.

For the quasi-steady state flow, one has

$$R_C = Q/(2\pi Bq_C), \quad (2)$$

where  $B$  is the thickness of the aquifer (L);  $Q$  is the well discharge ( $L^3T^{-1}$ ). For the case with a constant pumping rate,  $R_C$  is also a constant for a specific  $Re_C$ . This constant  $R_C$  was used in previous two-region models of transient non-Darcian flow (Sen, 1988; Wen et al., 2008b). Actually,  $R_C$  is not a constant for transient flow, and it cannot be determined directly since the velocity distribution changes with time. In this study, a new iteration method will be proposed to determine  $R_C$  as described below.

## 2.2 Mathematic model

Figure 1 shows the physical model investigated in this study, where a pumping well fully penetrates a confined aquifer. The origin of the cylindrical coordinate system is at the center of the well. The  $r$  axis is horizontal and outward from the well, and the  $z$  axis is upward vertical. Two assumptions are made in this study. First, the non-Darcian and Darcian flow may coexist and the critical radius is time-dependent, and the non-Darcian flow is governed by the Forchheimer law. Second, the system is hydrostatic before the pumping starts, so  $R_C(t = 0) = 0$ . These assumptions, although quite idealized, are standard in well hydraulic study (Papadopoulos and Cooper, 1967; Sen, 1988; Wen et al., 2008b). Based on these assumptions, the governing equations of the two-region flow model can be described as follows

$$\frac{\partial q_N(r,t)}{\partial r} + \frac{q_N(r,t)}{r} = \frac{S}{B} \frac{\partial s_N(r,t)}{\partial t}, \quad \text{if } r \leq R_C(t), \quad (3)$$

$$\frac{\partial q_Y(r,t)}{\partial r} + \frac{q_Y(r,t)}{r} = \frac{S}{B} \frac{\partial s_Y(r,t)}{\partial t}, \quad \text{if } r > R_C(t), \quad (4)$$

where  $s_Y(r,t)$  and  $s_N(r,t)$  are drawdowns (L) at distance  $r$  and time  $t$  in Darcian flow and non-Darcian flow regions, respectively;  $S$  is the aquifer storage coefficient (dimensionless).

Title Page

Abstract

Introduction

Conclusions

References

Tables

Figures

⏪

⏩

◀

▶

Back

Close

Full Screen / Esc

Printer-friendly Version

Interactive Discussion





in which  $\beta$  ( $TL^{-1}$ ) and  $K_\beta$  ( $LT^{-1}$ ) are empirical constants depending on the properties of the medium (Sidiropoulou et al., 2007).  $\beta$  is called the inertial force coefficient.  $K_\beta$  is called the apparent hydraulic conductivity and it reduces to the hydraulic conductivity when  $\beta = 0$  (Chen et al., 2001; Sidiropoulou et al., 2007).

5 In the Darcian flow region, one has

$$q_Y(r,t) = K \frac{\partial s_Y(r,t)}{\partial r}, \quad r > R_C. \quad (12)$$

Equations (3–12) compose of the mathematical model of the two-region model with a time-dependent critical radius  $R_C(t)$ . This new model is an extension of the previous model by Sen (1988). When  $R_C(t) \rightarrow \infty$ , this model becomes the F-ND model. When  
 10  $R_C(t) = 0$ , it reduces to the fully Darcian flow model.

### 2.3 Dimensionless transformation

Defining the dimensionless variables in Table 1, Eqs. (3–12) can be rewritten as

$$\frac{\partial q_{ND}}{\partial r_D} + \frac{q_{ND}}{r_D} = -\frac{\partial s_{ND}}{\partial t_D}, \quad r_D \leq R_{CD}, \quad (13)$$

$$\frac{\partial q_{YD}}{\partial r_D} + \frac{q_{YD}}{r_D} = -\frac{\partial s_{YD}}{\partial t_D}, \quad r_D > R_{CD}, \quad (14)$$

$$15 \quad s_{ND}(r_D, 0) = s_{YD}(r_D, 0) = 0, \quad (15)$$

$$s_{YD}(\infty, t_D) = 0, \quad (16)$$

$$s_{ND}[R_{CD}(t_D), t_D] = s_{YD}[R_{CD}(t_D), t_D], \quad (17)$$

$$q_{ND}[R_{CD}(t_D), t_D] = q_{YD}[R_{CD}(t_D), t_D]. \quad (18)$$

20 Notice that a negative sign has been used for defining  $q_D$  in Table 1. The subscript D means the dimensionless variables. The boundary condition with the wellbore storage

(Eq. 7) in the dimensionless form is

$$(r_D q_{ND})|_{r_D \rightarrow r_{wD}} + \frac{r_{wD}^2}{2S} \frac{ds_{wD}(t_D)}{dt_D} = 1. \quad (19)$$

The dimensionless Forchheimer law becomes

$$q_{ND} + \beta_D q_{ND} |q_{ND}| = -\frac{\partial s_{ND}}{\partial r_D}, \quad r_D \leq R_{CD}, \quad (20)$$

5 where  $\beta_D$  is the dimensionless inertial force coefficient. When  $r_D > R_{CD}$ , groundwater flow follows the Darcy's law in the dimensionless format as

$$q_{YD}(r, t) = -\lambda \frac{\partial s_{YD}}{\partial r_D}, \quad r_D > R_{CD}, \quad (21)$$

where  $\lambda$  is the ratio of the hydraulic conductivity and apparent hydraulic conductivity, and it is usually taken as unity (Sidiropoulou et al., 2007).

### 10 3 Numerical solution

Because of the non-linearity of the problem, it is not easy to obtain the analytical solution of drawdown even if  $R_{CD}(t_D)$  is constant. In this study, we will employ the finite-difference method to investigate the problem considering a time-dependent  $R_{CD}(t_D)$ . Due to the axisymmetric nature of the problem, the numerical simulation will be conducted with a non-uniform grid system, where the radial steps are smaller near the well and become progressively greater away from the well. Similar to previous studies (Mathias et al., 2008; Wen et al., 2009), we discretize the dimensionless space  $r_D$  logarithmically. The dimensionless space domain  $[r_{wD}, r_{eD}]$  is discretized into  $N$  nodes excluding the two boundary nodes  $r_{wD}$  and  $r_{eD}$ , where  $r_{eD}$  is a relatively large dimensionless distance used to approximate the infinite boundary (Mathias et al., 2008; Wen

Title Page

Abstract

Introduction

Conclusions

References

Tables

Figures

⏪

⏩

◀

▶

Back

Close

Full Screen / Esc

Printer-friendly Version

Interactive Discussion



et al., 2009). For any node of  $r_i$ ,  $r_{wD} < r_i < r_{eD}$ ,  $i = 1, 2, \dots, N$ , one has

$$r_i = (r_{i-1/2} + r_{i+1/2})/2, \quad i = 1, 2, \dots, N, \quad (22)$$

where  $r_{i+1/2}$  is calculated as follows

$$\log_{10}(r_{i+1/2}) = \log_{10}(r_{wD}) + i \left[ \frac{\log_{10}(r_{eD}) - \log_{10}(r_{wD})}{N} \right], \quad i = 0, 1, \dots, N. \quad (23)$$

5 After the spatial discretization, Eqs. (13) and (14) become

$$\frac{ds_{YD,i}}{dt_D} \approx \frac{r_{i-1/2}q_{YD,i-1/2} - r_{i+1/2}q_{YD,i+1/2}}{r_i(r_{i+1/2} - r_{i-1/2})}, \quad i = 2, 3, \dots, N_s - 1, \quad r_D \leq R_{CD}, \quad (24)$$

$$\frac{ds_{ND,i}}{dt_D} \approx \frac{r_{i-1/2}q_{ND,i-1/2} - r_{i+1/2}q_{ND,i+1/2}}{r_i(r_{i+1/2} - r_{i-1/2})}, \quad i = N_s, 3, \dots, N - 1, \quad r_D > R_{CD}, \quad (25)$$

10 where  $q_{YD,i}$  and  $s_{YD,i}$  are the dimensionless specific discharge  $q_{YD}$  and dimensionless drawdown  $s_{YD}$  at node  $i$  for the Darcian flow, respectively;  $q_{ND,i}$  and  $s_{ND,i}$  are the dimensionless specific discharge  $q_{ND}$  and dimensionless drawdown  $s_{ND}$  at node  $i$  for the non-Darcian flow, respectively. In terms of the Forchheimer equation of Eq. (20), one can obtain

$$q_{ND,i-1/2} \approx \frac{1}{2\beta_D} \left\{ -1 + \left[ 1 + 4\beta_D \left( \frac{s_{ND,i-1} - s_{ND,i}}{r_i - r_{i-1}} \right) \right]^{\frac{1}{2}} \right\}, \quad i = 2, 3, \dots, N_s - 1, \quad (26)$$

15 and

$$q_{ND,i+1/2} \approx \frac{1}{2\beta_D} \left\{ -1 + \left[ 1 + 4\beta_D \left( \frac{s_{ND,i} - s_{ND,i+1}}{r_{i+1} - r_i} \right) \right]^{\frac{1}{2}} \right\}, \quad i = 2, 3, \dots, N_s - 1, \quad (27)$$

where node  $N_s$  means the location of  $R_{CD}(t_D)$ . At the well-aquifer boundary, one has

$$q_{ND,1-1/2} \approx \frac{1}{2\beta_D} \left\{ -1 + \left[ 1 + 4\beta_D \left( \frac{s_{wD} - s_{ND,1}}{r_1 - r_{wD}} \right) \right]^{\frac{1}{2}} \right\}, \quad (28)$$

where  $s_{wD}$  is the dimensionless drawdown inside the well. Considering Eq. (19),  $s_{wD}$  can be approximated as follows

$$\frac{ds_{wD}}{dt_D} \approx \frac{2S}{r_{wD}^2} (1 - r_{wD} q_{ND,1-1/2}). \quad (29)$$

When  $r_D > R_{CD}$ , the finite-difference scheme of the specific discharge can be obtained from Eq. (21):

$$q_{YD,i-1/2} \approx \lambda \frac{s_{YD,i-1} - s_{YD,i}}{r_i - r_{i-1}}, \quad i = N_s, N_s + 1, \dots, N - 1, \quad (30)$$

$$q_{YD,i+1/2} \approx \lambda \frac{s_{YD,i} - s_{YD,i+1}}{r_{i+1} - r_i}, \quad i = N_s, N_s + 1, \dots, N - 1. \quad (31)$$

As for the boundary at the infinity, the finite-difference scheme is

$$q_{YD,N+1/2} \approx \lambda \frac{s_{YD,N}}{r_{eD} - r_N}. \quad (32)$$

Now one obtains a set of ordinary differential equations. It is notable that  $R_{CD}$  or  $N_s$  which is related to the index  $i$  in Eqs. (26) and (27) and Eqs. (30) and (31) is time-dependent. In the following section, a new iteration method will be proposed to determine the values of  $R_{CD}$  or  $N_s$ .

## HESSD

10, 14095–14129, 2013

### Forchheimer flow to a well considering time-dependent critical radius

Q. Wang et al.

Title Page

Abstract

Introduction

Conclusions

References

Tables

Figures

⏪

⏩

◀

▶

Back

Close

Full Screen / Esc

Printer-friendly Version

Interactive Discussion

#### 4 Iteration method to determine $R_{CD}$ or $N_s$

Before introducing the new iteration method, the relationship between  $R_{CD}$  and the velocity distribution will be investigated first, based on the two-region model with a constant  $R_{CD}$ . The values of the constant  $R_{CD}$  are set as 0, 0.02, 0.04, 0.08 and 0.50, respectively. The other parameters are  $r_{wD} = 1 \times 10^{-5}$ ,  $\beta_D = 20$ ,  $\lambda = 1$ . The mathematic model with a constant  $R_{CD}$  will be solved by the finite-difference method.

Figure 2a shows the specific discharge distributions with different  $R_{CD}$  of 0, 0.02, 0.04, 0.08 and 0.50. The curve of  $R_{CD} = 0$  represents the fully Darcian flow model. One can find that the specific discharge decreases with increasing  $R_{CD}$  at a given  $r_D$ , starting from its maximum at  $R_{CD} = 0$  (Darcian flow). This observation is understandable. The increasing  $R_{CD}$  implies a stronger contribution of the inertial effect, which also means a larger resistance to flow, thus it leads to a smaller specific discharge. After trying many different sets of aquifer parameters, numerical simulation indicates that this observation is universally valid. This observation will serve as the basis for the new iteration method to seek the location of  $R_{CD}(t_D)$ .

Similar to the use of  $Re_C$  to determine the start of the non-Darcian flow, one can use  $q_{CD}$  for the initiation of the non-Darcian flow, where  $q_{CD}$  is the dimensionless critical specific discharge defined in Table 1. We denote  $r_{jCD}$  as the newly computed critical radius at the  $j$ th step of the new iteration method, where  $j = 1, 2, 3, \dots$ . Since the aquifer system is initially hydrostatic, the initial critical radius  $r_{0CD}$  is set as 0. For a given dimensionless time  $t_{1D}$ , the detailed procedures of the iteration method for searching  $R_{CD}(t_{1D})$  will be introduced as follows. Firstly, the specific discharge distribution in the aquifer can be calculated using Eqs. (24–32) with  $R_{CD}(t_{1D}) = r_{0CD}$ , as shown in Fig. 2b. Based on the computed specific discharge distribution, one can find the new critical radius  $r_{1CD}$  according to a given constant  $q_{CD}$ . Secondly, the new specific discharge distribution can be similarly calculated using Eqs. (24–32) with  $R_{CD}(t_{1D}) = r_{1CD}$ , and the new critical radius  $r_{2CD}$  can be obtained according to  $q_{CD}$ . It is notable that  $r_{1CD}$  and  $r_{2CD}$  serve as the upper and lower limits for searching  $R_{CD}(t_{1D})$ , as illustrated in

## HESSD

10, 14095–14129, 2013

### Forchheimer flow to a well considering time-dependent critical radius

Q. Wang et al.

Title Page

Abstract

Introduction

Conclusions

References

Tables

Figures

⏪

⏩

◀

▶

Back

Close

Full Screen / Esc

Printer-friendly Version

Interactive Discussion



## Forchheimer flow to a well considering time-dependent critical radius

Q. Wang et al.

$$q_{YD}(r_D, t_D) = F(r_{cD}, t_D) \exp \left[ \frac{r_{cD}^2 (1 - \lambda)}{4\lambda t_D} \right] \frac{\exp \left( -\frac{r_D^2}{4t_D \lambda} \right)}{r_D}, \quad (34)$$

where  $F(r_D, t_D) = \frac{1}{1 + \frac{\sqrt{\pi} \beta_D}{2} \left( \frac{1}{t_D} \right)^{1/2} \operatorname{erf} \left[ \left( \frac{r_D^2}{4t_D} \right)^{1/2} \right]}$ , and erf is the error function sign.

5 In the non-Darcian flow region ( $r_D < R_{cD}$ ),

$$s_{ND}(r_D, t_D) = s_{YD}(r_{cD}, t_D) + \int_{r_D}^{r_{cD}} F(\zeta, t_D) \frac{\exp \left( -\frac{\zeta^2}{4t_D} \right)}{\zeta} d\zeta \quad (35)$$

$$+ \beta_D \int_{r_D}^{r_{cD}} F^2(\zeta, t_D) \frac{\exp \left( -\frac{\zeta^2}{2t_D} \right)}{\zeta^2} d\zeta,$$

$$q_{ND}(r_D, t_D) = F(r_D, t_D) \frac{\exp \left( -\frac{r_D^2}{4t_D} \right)}{r_D}. \quad (36)$$

10 Figures 4a and b show the distance-drawdown curves in the early and late pumping stages, respectively. In these two figures, Papadopoulos and Cooper (1967) represents the analytical solution of the fully Darcian flow model, Sen (1988) is the analytical solution of the two-region model by the Boltzmann transform method, and Mathias et al. (2008) represents the numerical solution of the fully non-Darcian flow model. The deflection point of the curve is the location of the critical radius.

15 In the early stage, the differences among three previous solutions and the new solution of this study are obvious, as shown in Fig. 4a. Firstly, the solution of Papadopoulos and Cooper (1967) is smaller than the others near the well. This is because the inertial

[Title Page](#)
[Abstract](#)
[Introduction](#)
[Conclusions](#)
[References](#)
[Tables](#)
[Figures](#)
[⏪](#)
[⏩](#)
[◀](#)
[▶](#)
[Back](#)
[Close](#)
[Full Screen / Esc](#)
[Printer-friendly Version](#)
[Interactive Discussion](#)



## Forchheimer flow to a well considering time-dependent critical radius

Q. Wang et al.

Title Page

Abstract

Introduction

Conclusions

References

Tables

Figures

⏪

⏩

◀

▶

Back

Close

Full Screen / Esc

Printer-friendly Version

Interactive Discussion



time until the flow approaching the quasi-steady state condition. In the early pumping stage, the specific discharge is very large near the well and decreases quickly with the distance from the well, so  $R_{CD}$  is very small. With time going, the cone of depression will expand along the radial direction and the slope of the cone of depression becomes flatter, so  $R_{CD}$  becomes greater. Secondly, a larger  $\beta_D$  would reduce the rate of change  $R_{CD}$  vs. time, thus result in longer time to approach its asymptotic value, and consequently leads to a smaller  $R_{CD}$  at a specific time in the transient state (see Fig. 5). This is because that a larger  $\beta_D$  implies a stronger inertial force, which increases the resistance of flow. The third interesting observation is that the asymptotic value of  $R_{CD}$  is the same for different  $\beta_D$ . This can be explained using Eq. (2). Based on the definition of the dimensionless parameters defined in Table 1, Eq. (2) becomes

$$q_{CD} = 1/R_{CD}. \quad (37)$$

Therefore, the value of  $R_{CD}$  has no relationship with  $\beta_D$  under the quasi-state state flow condition, while it only reciprocally depends on the critical specific discharge.

### 5.3 Effect of the critical specific discharge to the critical radius

The criterion to judge the initiation of the non-Darcian flow is an important factor of concern. Up to now, there is still considerable debate on what value of  $Re_C$  to use for the start of non-Darcian low. The recommended values of  $Re_C$  range from 0.1 to 100 for porous media flow (Bear, 1972; Scheidegger, 1974; Zeng and Grigg, 2006). To check the influence of  $Re_C$  on  $R_{CD}$  during the transient flow, the values of  $q_{CD}$  are chosen as 1, 2 and 5 considering the direct relationship of  $q_{CD}$  and  $R_{CD}$  in Eq. (2). The other parameters are  $\beta_D = 1$ , and  $r_{wD} = 1 \times 10^{-4}$ .

Figure 6 represents the effect of  $q_{CD}$  on  $R_{CD}$ . It is obvious that the asymptotic value of  $R_{CD}$  is equal to  $1/q_{CD}$ , as reflected in Eq. (37). Another interesting observation is that  $R_{CD}$  decreases with increasing  $q_{CD}$ , and it takes shorter time for  $R_{CD}$  to approach its asymptotic value. The reason can be also explained using Eq. (37).

## 5.4 Type curves in the non-Darcian flow region and Darcian flow region

Type curves are a series of curves that reveal the functional relationship between the well functions (or drawdown) and the dimensionless time factors (Sen, 1988; Wen et al., 2011). Type curve is one of the common approaches to identify the aquifer parameters or to predict the drawdown (Sen, 1988; Wen et al., 2011). Sen (1988) presented different type curves in the Darcian flow region and non-Darcian flow region based on a two-region model. In that model (Sen, 1988),  $R_{CD}$  was a fixed value which only depends on the rate of pumping but independent of time. In this study,  $R_{CD}$  changes with time, and the type curves might be different from the ones generated by Sen (1988). To investigate the behaviors of the type curves of the new solution, the value of  $q_{CD}$  is set to be 2, and the two observation locations will be chosen,  $r_D = 0.1$  and 1.0. According to Eq. (37), the maximum of  $R_{CD}$  is 0.5 at the quasi-steady state, so the flow at  $r_D = 0.1$  will experience both Darcian flow (at the early time) and non-Darcian flow (at late time), while the flow at  $r_D = 1.0$  is always Darcian.

Figure 7 shows the time-drawdown at  $r_D = 0.1$  for different dimensionless inertial force coefficients in the log-log scale. Two interesting observations can be seen from this figure. The first observation is that there is a deflection point in the curve, and the time of this deflection point becomes longer with increasing  $\beta_D$ . This is because a larger  $\beta_D$  implies a stronger inertial effect, which leads to a larger drawdown and longer time to approach the quasi-steady state condition. This observation is not found in the F-ND model (Wen et al., 2011) and in the two-region model (Sen, 1988). The second observation is that the drawdown in the quasi-steady state increases with increasing  $\beta_D$ , and the reason for this has been explained in previous studies (Wen et al., 2011).

Figure 8 represents the time-drawdown at  $r_D = 1$  in the semi-log scale. One notable point is that flow at  $r_D = 1$  is always Darcian, so there is no deflection point in the type curves. The differences among the curves with different  $\beta_D$  are very small at the beginning, then they become larger with time going, and finally approach the same value at the quasi-steady state. This is because the specific discharge far from the well

HESSD

10, 14095–14129, 2013

**Forchheimer flow to a well considering time-dependent critical radius**

Q. Wang et al.

Title Page

Abstract

Introduction

Conclusions

References

Tables

Figures

⏪

⏩

◀

▶

Back

Close

Full Screen / Esc

Printer-friendly Version

Interactive Discussion

is very small at the beginning, so the drawdown approaches 0. With time going, the inertial force affects the groundwater flow at  $r_D = 0.1$ . At the quasi-steady state, the drawdown in the Darcian flow region does not change with  $\beta_D$ , where the reason has been explained in Sect. 5.1, as shown in Fig. 4b.

## 6 Summary and conclusions

In this study, a new two-region flow model considering the time-dependent critical radius ( $R_{CD}$ ) is established to investigate the groundwater flow into a pumping well, and a new iteration method is proposed to estimate  $R_{CD}$ , based on the finite-difference method. The convergence of this iteration method has been verified. In the non-Darcian flow region, the flow is governed by the Forchheimer equation, and the start of the non-Darcian flow is determined by the critical specific discharge, which is calculated by the critical Reynolds number. The new solution is compared with previous solutions, such as the fully Darcian flow model, the two-region model with a constant critical radius, and the fully non-Darcian flow model. The impacts of the dimensionless inertial force coefficient ( $\beta_D$ ) and dimensionless critical specific discharge ( $q_{CD}$ ) on the critical radius and flow field have been analyzed. Several findings can be drawn from this study:

1. In the early stage, the new solution agrees with the fully non-Darcian flow solution near the well, differs with the fully Darcian flow model of Papadopoulos and Cooper (1967) and the two-region model of Sen (1988).
2. In the quasi-steady flow stage, the new solution agrees with the solution of Sen (1988) very well. It agrees very well with the solution of the fully Darcian flow model (Papadopoulos and Cooper, 1967) in the Darcian flow region, and with the solution of the fully non-Darcian flow model (Mathias et al., 2008) in the non-Darcian flow region near the well.
3.  $R_{CD}$  increases with time until reaching the quasi-steady state flow, and the asymptotic value of  $R_{CD}$  only depends on  $q_{CD}$ . A larger  $\beta_D$  would reduce the rate of

## Forchheimer flow to a well considering time-dependent critical radius

Q. Wang et al.

Title Page

Abstract

Introduction

Conclusions

References

Tables

Figures

⏪

⏩

◀

▶

Back

Close

Full Screen / Esc

Printer-friendly Version

Interactive Discussion



change of  $R_{CD}$  with time, and result in a smaller  $R_{CD}$  at a specific time during the transient flow state.

4. There is a deflection point in the type curve when the observation well location is within the non-Darcian flow region in the quasi-steady state, and the time associated with this deflection point becomes longer with a larger  $\beta_D$ .

*Acknowledgements.* This research was partially supported by Program of the National Basic Research Program of China (973) (No. 2011CB710600, 2011CB710602), National Natural Science Foundation of China (No. 41172281, 41372253), and the scholarship to Quanrong Wang from China Scholarship Council (CSC), Field Demonstration of Integrated Monitoring Program of Land and Resources in Middle Yangtze River Jiangnan-Dongtin Plain (1212011120084).

## References

- Ahmad, N.: Evaluation of groundwater resources in the upper middle part of Chaj-Doak area, Pakistan., PhD, Istanbul Technical Univ., Turkey, 1998.
- Basak, P.: Non-penetrating well in a semi-infinite medium with nonlinear flow, *J. Hydrol.*, **33**, 375–382, doi:10.1016/0022-1694(77)90047-6, 1977.
- Basak, P.: Analytical solutions for two-regime well flow problems, *J. Hydrol.*, **38**, 147–159, 1978.
- Bear, J.: *Dynamics of Fluids in Porous Media*, Elsevier, New York, 1972.
- Birpinar, M. E. and Sen, Z.: Forchheimer groundwater flow law type curves for leaky aquifers, *J. Hydrol. Eng.*, **9**, 51–59, doi:10.1061/(ASCE)1084-0699(2004)9:1(51), 2004.
- Bordier, C. and Zimmer, D.: Drainage equations and non-Darcian modelling in coarse porous media or geosynthetic materials, *J. Hydrol.*, **228**, 174–187, doi:10.1016/s0022-1694(00)00151-7, 2000.
- Camacho, R. G. and Vasquez, M.: Analytical solution incorporating nonlinear radial flow in confined aquifers – comment, *Water Resour. Res.*, **28**, 3337–3338, doi:10.1029/92wr01646, 1992.
- Chen, Z. X., Lyons, S. L., and Qin, G.: Derivation of the Forchheimer law via homogenization, *Transp. Por. Media*, **44**, 325–335, doi:10.1023/a:1010749114251, 2001.

Title Page

Abstract

Introduction

Conclusions

References

Tables

Figures

⏪

⏩

◀

▶

Back

Close

Full Screen / Esc

Printer-friendly Version

Interactive Discussion





## Forchheimer flow to a well considering time-dependent critical radius

Q. Wang et al.

[Title Page](#)

[Abstract](#)

[Introduction](#)

[Conclusions](#)

[References](#)

[Tables](#)

[Figures](#)

[⏪](#)

[⏩](#)

[◀](#)

[▶](#)

[Back](#)

[Close](#)

[Full Screen / Esc](#)

[Printer-friendly Version](#)

[Interactive Discussion](#)



Mathias, S. A., Butler, A. P., and Zhan, H. B.: Approximate solutions for Forchheimer flow to a well, *J. Hydraul. Eng.-ASCE*, 134, 1318–1325, doi:10.1061/(asce)0733-9429(2008)134:9(1318), 2008.

Mathias, S. A. and Todman, L. C.: Step-drawdown tests and the Forchheimer equation, *Water Resour. Res.*, 46, W07514, doi:10.1029/2009wr008635, 2010.

Mishra, P. K., Vessilinov, V., and Gupta, H.: On Simulation and Analysis of Variable-Rate Pumping Tests, *Ground Water*, 51, 469–473, doi:10.1111/j.1745-6584.2012.00961.x, 2012.

Papadopoulos, I. S. and Cooper, H. H.: Drawdown in a well of large diameter, *Water Resour. Res.*, 3, 241–244, doi:10.1029/WR003i001p00241, 1967.

Quinn, P. M., Parker, B. L., and Cherry, J. A.: Validation of non-Darcian flow effects in slug tests conducted in fractured rock boreholes, *J. Hydrol.*, 486, 505–518, doi:10.1016/j.jhydrol.2013.02.024, 2013.

Scheidegger, A. E.: *The Physics of Flow through Porous Media*, University of Toronto Press, 152–170, 1974.

Sen, Z.: Type curves for two-region well flow, *J. Hydraul. Eng.*, 114, 1461–1484, doi:10.1029/WR024i004p00601, 1988.

Sen, Z.: Nonlinear radial flow in confined aquifers toward large-diameter wells, *Water Resour. Res.*, 26, 1103–1109, doi:10.1029/WR026i005p01103, 1990.

Sen, Z.: Non-Darcian groundwater flow in leaky aquifers, *Hydrolog. Sci. J.*, 45, 595–606, doi:10.1080/02626660009492360, 2000.

Sidiropoulou, M. G., Moutsopoulos, K. N., and Tsihrintzis, V. A.: Determination of Forchheimer equation coefficients  $a$  and  $b$ , *Hydrol. Process.*, 21, 534–554, doi:10.1002/hyp.6264, 2007.

Soni, J. P., Islam, N., and Basak, P.: Experimental evaluation of non-Darcian flow in porous media, *J. Hydrol.*, 38, 231–241, doi:10.1016/0022-1694(78)90070-7, 1978.

van Tonder, G. J., Botha, J. F., and van Bosch, J.: A generalised solution for step-drawdown tests including flow dimension and elasticity, *Water S. A.*, 27, 345–354, 2001.

Ward, J. C.: Turbulent flow in porous media, *J. Hydraul. Div.-ASCE*, 90, 1–12, 1964.

Wen, Z., Huang, G. H., and Zhan, H. B.: An analytical solution for non-Darcian flow in a confined aquifer using the power law function, *Adv. Water Resour.*, 31, 44–55, doi:10.1016/j.advwatres.2007.06.002, 2008a.

Wen, Z., Huang, G. H., Zhan, H. B., and Li, J.: Two-region non-Darcian flow toward a well in a confined aquifer, *Adv. Water Resour.*, 31, 818–827, doi:10.1016/j.advwatres.2008.01.014, 2008b.

# HESSD

10, 14095–14129, 2013

## Forchheimer flow to a well considering time-dependent critical radius

Q. Wang et al.

Title Page

Abstract

Introduction

Conclusions

References

Tables

Figures



Back

Close

Full Screen / Esc

Printer-friendly Version

Interactive Discussion



- Wen, Z., Huang, G. H., and Zhan, H. B.: A numerical solution for non-Darcian flow to a well in a confined aquifer using the power law function, *J. Hydrol.*, 364, 99–106, doi:10.1016/j.jhydrol.2008.10.009, 2009.
- 5 Wen, Z., Huang, G. H., and Zhan, H. B.: Non-Darcian flow to a well in a leaky aquifer using the Forchheimer equation, *Hydrogeol. J.*, 19, 563–572, doi:10.1007/s10040-011-0709-2, 2011.
- Whitaker, S.: The Forchheimer equation: a theoretical development, *Transp. Por. Media*, 25, 27–61, doi:10.1007/bf00141261, 1996.
- Yeh, H.-D. and Chang, Y.-C.: Recent advances in modeling of well hydraulics, *Adv. Water Resour.*, 51, 27–51, doi:10.1016/j.advwatres.2012.03.006, 2013.
- 10 Zeng, Z. W. and Grigg, R.: A criterion for non-Darcy flow in porous media, *Transp. Por. Media*, 63, 57–69, doi:10.1007/s11242-005-2720-3, 2006.

## Forchheimer flow to a well considering time-dependent critical radius

Q. Wang et al.

**Table 1.** Dimensionless variables used in this study.

$r_D = \frac{r}{B}$	$r_{wD} = \frac{r_w}{B}$
$R_{CD} = \frac{R_C}{B}$	$t_D = \frac{K_\beta t}{SB}$
$\beta_D = \frac{Q\beta}{2\pi B^2}$	$\lambda = \frac{K}{K_\beta}$
$s_{wD} = \frac{2\pi K_\beta B}{Q} s_w$	$s_{yD} = \frac{2\pi K_\beta B}{Q} s_Y(r, t)$
$s_{nD} = \frac{2\pi K_\beta B}{Q} s_N(r, t)$	$q_{nD} = -\frac{2\pi B^2}{Q} q_N(r, t)$
$q_{yD} = -\frac{2\pi B^2}{Q} q_Y(r, t)$	$q_{cD} = -\frac{2\pi B^2}{Q} q_C$

Title Page

Abstract

Introduction

Conclusions

References

Tables

Figures

◀

▶

◀

▶

Back

Close

Full Screen / Esc

Printer-friendly Version

Interactive Discussion

## Forchheimer flow to a well considering time-dependent critical radius

Q. Wang et al.

Title Page

Abstract

Introduction

Conclusions

References

Tables

Figures

⏪

⏩

◀

▶

Back

Close

Full Screen / Esc

Printer-friendly Version

Interactive Discussion

**Table 2.** Nomenclature.

$B$	aquifer thickness (L)
$D_p$	characteristic grain diameter (L)
$K$	hydraulic conductivity of the aquifer ( $\text{LT}^{-1}$ )
$K_\beta$	apparent hydraulic conductivity, an empirical constant in the Forchheimer law ( $\text{LT}^{-1}$ )
$q$	specific discharge in the aquifer ( $\text{LT}^{-1}$ )
$q_C$	critical specific discharge ( $\text{LT}^{-1}$ )
$q_Y, q_N$	specific discharges for Darcian flow and non-Darcian flow ( $\text{LT}^{-1}$ ), respectively
$Q$	well discharge ( $\text{L}^3\text{T}^{-1}$ )
$s$	drawdown for aquifer (L)
$s_Y, s_N$	drawdowns for Darcian flow and non-Darcian flow (L), respectively
$s_w$	drawdown inside well (L)
$S$	storage coefficient of the aquifer (dimensionless)
$r$	distance from the center of the well (L)
$r_w$	radius of the well screen (L)
$R_C$	critical radius for non-Darcian flow (L)
$Re$	Reynolds number (dimensionless)
$Re_C$	critical Reynolds number (dimensionless)
$t$	pumping time (T)
$\beta$	an empirical constant in the Forchheimer law ( $\text{TL}^{-1}$ ), named as inertial force coefficient in this study
$\nu$	kinematic viscosity of the fluid ( $\text{L}^2\text{T}^{-1}$ )
$q_{ND}, q_{YD}$	dimensionless specific discharges defined in Table 1 in the non-Darcian flow and Darcian flow regions, respectively
$q_{CD}$	dimensionless critical specific discharge defined in Table 1
$r_D$	dimensionless distance defined in Table 1
$r_{wD}$	dimensionless radius of the well screen defined in Table 1
$R_{CD}$	dimensionless critical radius defined in Table 1
$s_{ND}, s_{YD}$	dimensionless drawdown $s$ defined in Table 1 in the non-Darcian flow and Darcian flow regions, respectively
$s_{wD}$	dimensionless drawdown inside the well defined in Table 1
$t_D$	dimensionless time defined in Table 1
$\beta_D$	dimensionless inertial force coefficient defined in Table 1
$\lambda$	ratio of the hydraulic conductivity and apparent hydraulic conductivity defined in Table 1

The subscript D refers to terms in dimensionless form.

The subscripts N and Y refer to terms related to non-Darcian flow and Darcian flow regions, respectively.

## Forchheimer flow to a well considering time-dependent critical radius

Q. Wang et al.

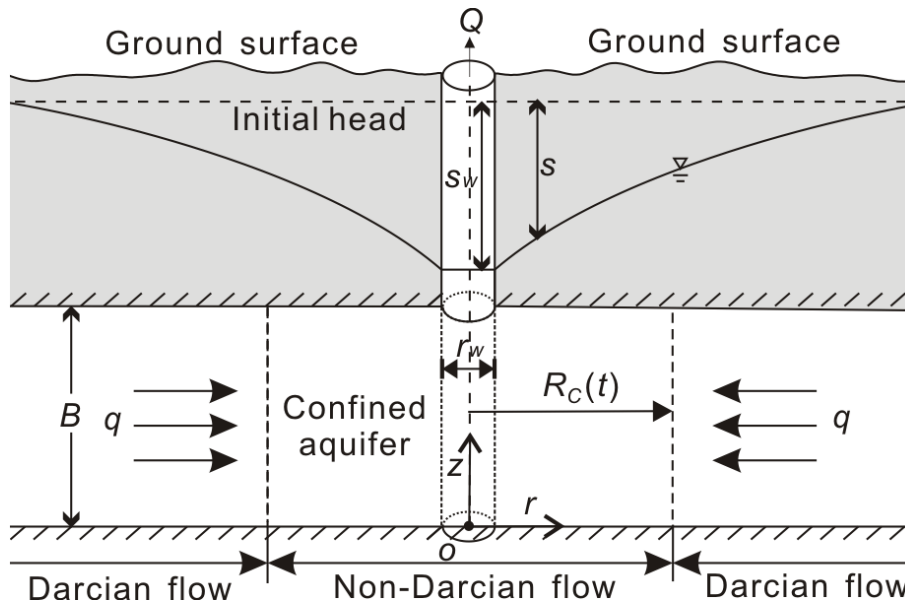


**Fig. 1.** The schematic diagram of the non-Darcian flow into a fully penetrating pumping well considering the time-dependent critical radius.

Title Page

Abstract

Introduction

Conclusions

References

Tables

Figures

◀

▶

◀

▶

Back

Close

Full Screen / Esc

Printer-friendly Version

Interactive Discussion

## Forchheimer flow to a well considering time-dependent critical radius

Q. Wang et al.

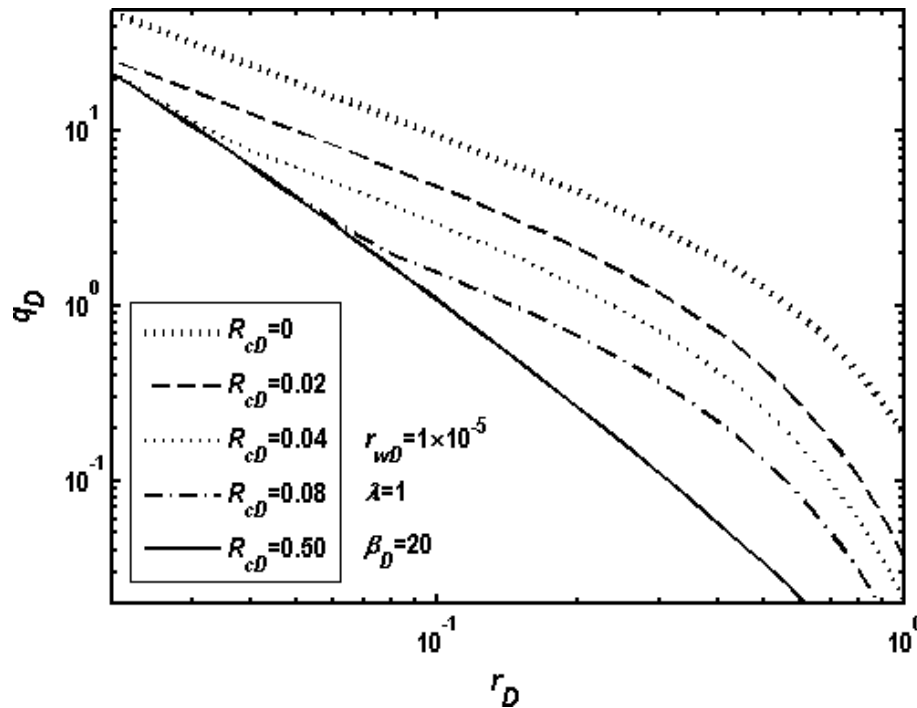


Fig. 2a. Specific discharge distributions with different critical radii  $R_{cD}$ .

Title Page

Abstract

Introduction

Conclusions

References

Tables

Figures

◀

▶

◀

▶

Back

Close

Full Screen / Esc

Printer-friendly Version

Interactive Discussion

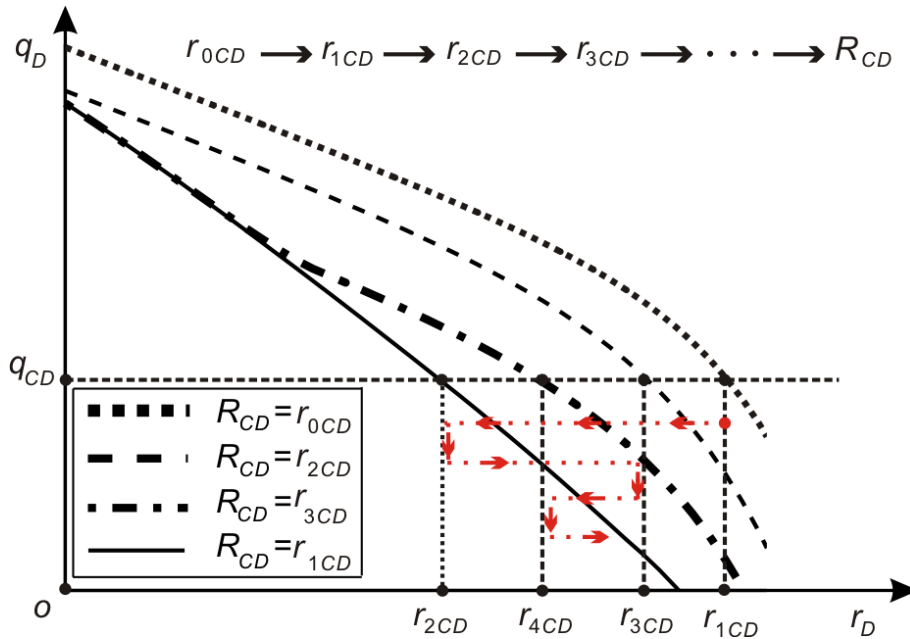


**Fig. 2b.** The schematic diagram showing the iterative process of seeking  $R_{CD}$ .

Title Page

Abstract	Introduction
Conclusions	References
Tables	Figures

⏪
⏩

◀
▶

Back	Close
------	-------

Full Screen / Esc

Printer-friendly Version

Interactive Discussion



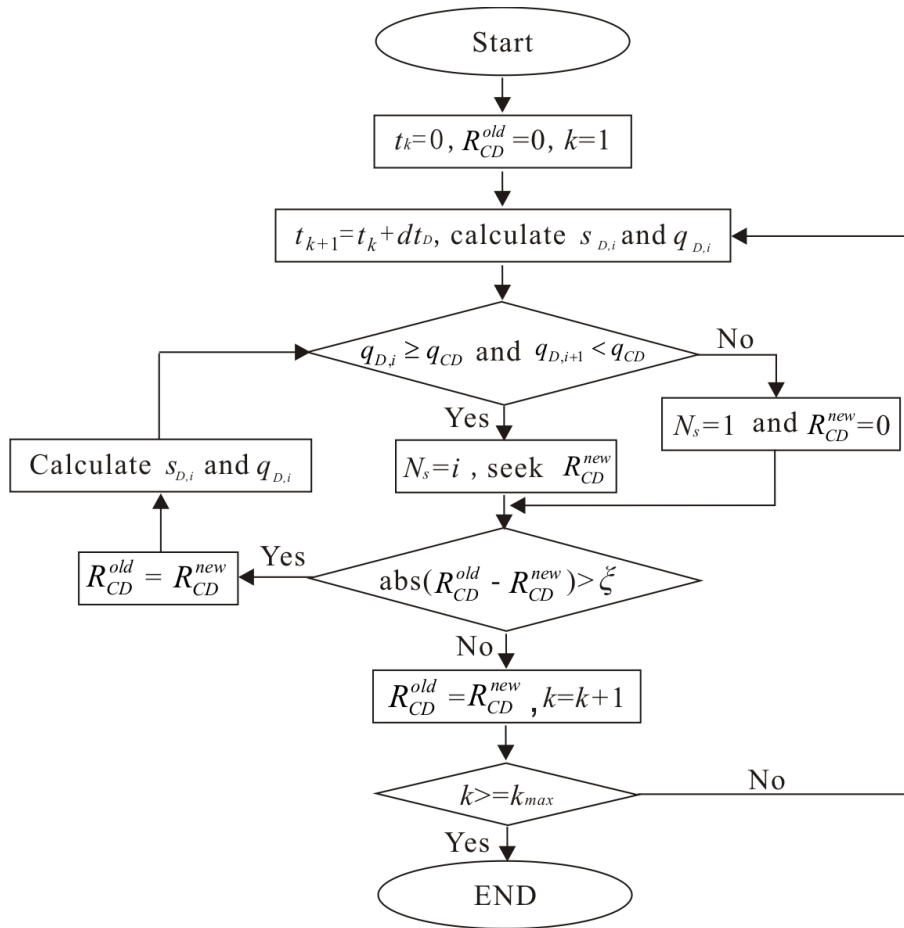


Fig. 3. Flow chat of the MTRM algorithm.

Title Page

Abstract Introduction

Conclusions References

Tables Figures

⏪ ⏩

◀ ▶

Back Close

Full Screen / Esc

Printer-friendly Version

Interactive Discussion



## Forchheimer flow to a well considering time-dependent critical radius

Q. Wang et al.

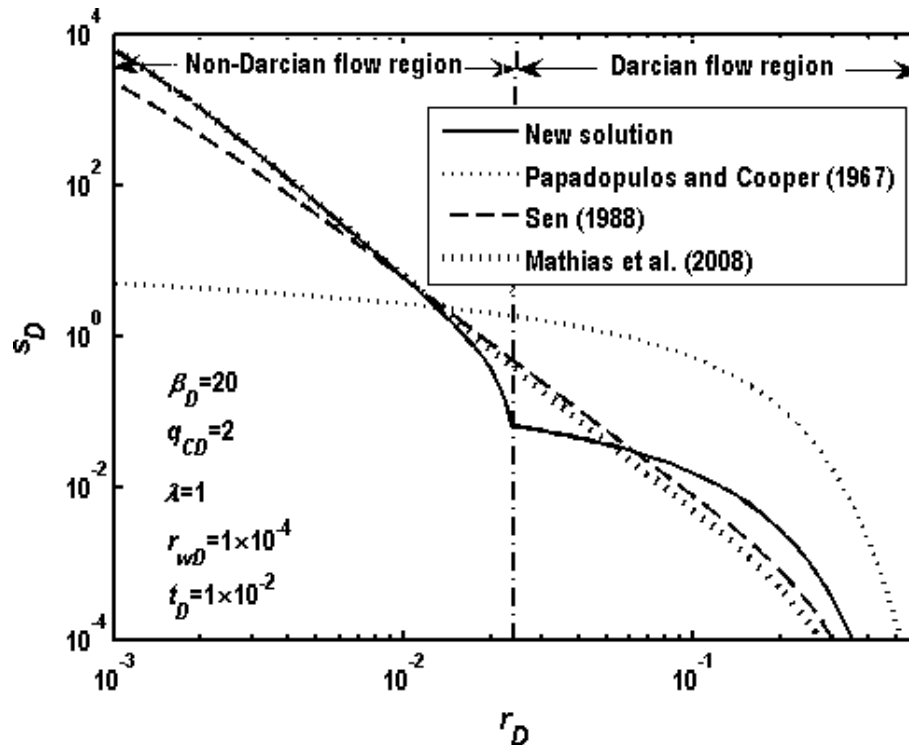


**Fig. 4a.** Comparison of the distance-drawdowns by the fully Darcian flow model, the fully non-Darcian flow model, the two-region flow model, and the new model in early pumping stage.

## Forchheimer flow to a well considering time-dependent critical radius

Q. Wang et al.

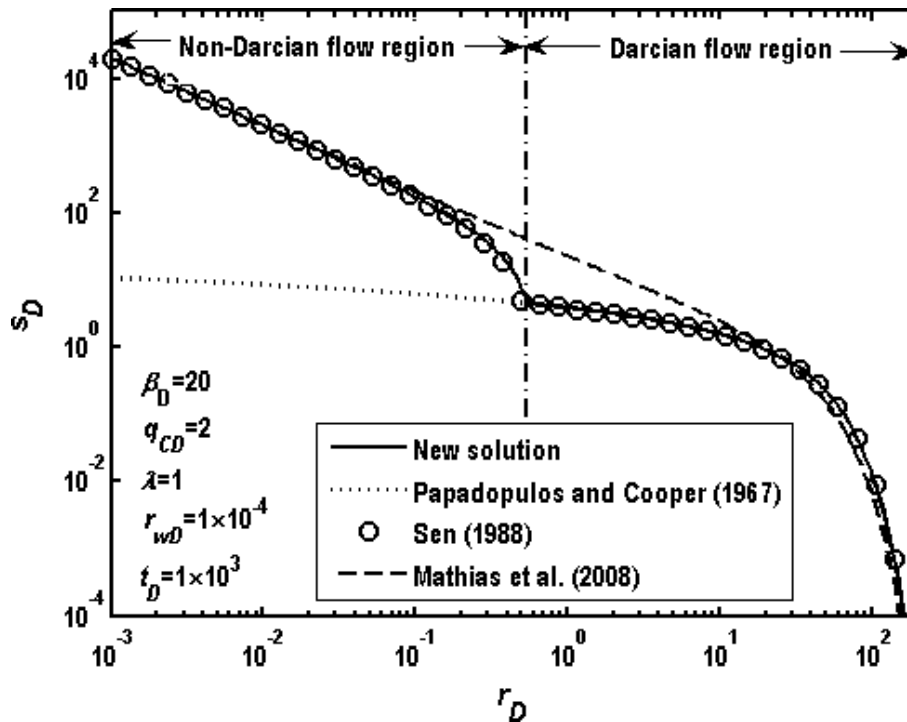


**Fig. 4b.** Comparison of the distance-drawdowns by the fully Darcian flow model, the fully non-Darcian flow model, the two-region model flow model, and the new model in late pumping stage.

Title Page

Abstract

Introduction

Conclusions

References

Tables

Figures

⏪

⏩

◀

▶

Back

Close

Full Screen / Esc

Printer-friendly Version

Interactive Discussion

**Forchheimer flow to a well considering time-dependent critical radius**

Q. Wang et al.

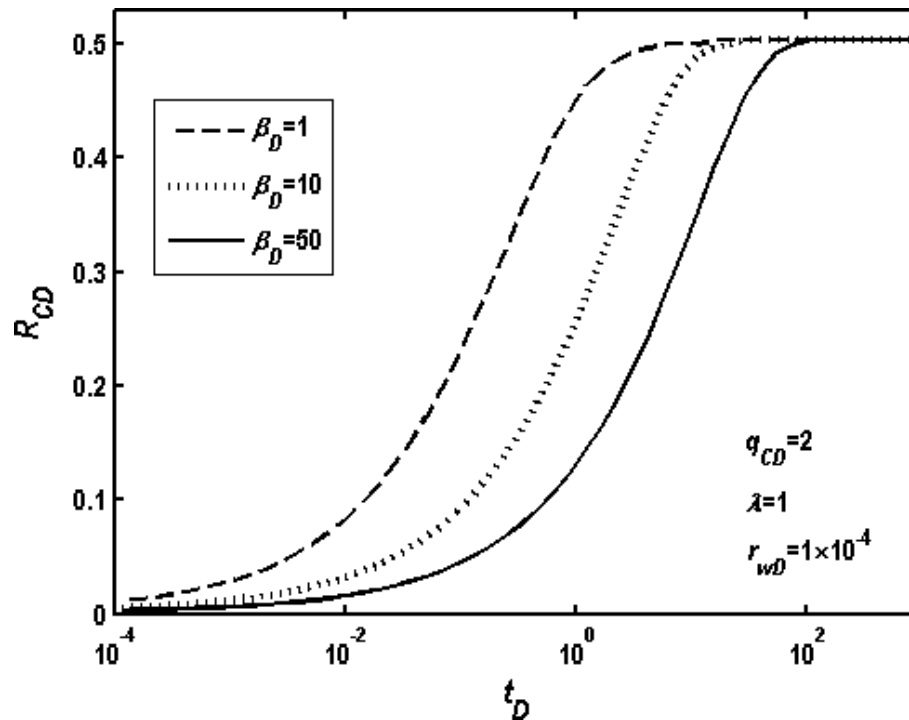
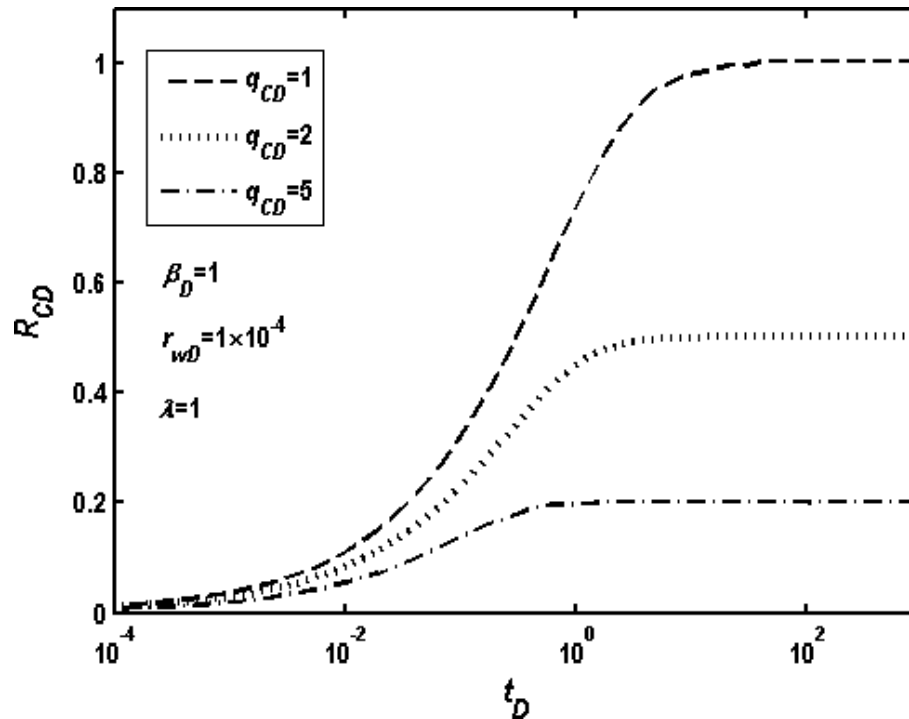


Fig. 5. Critical radius changes with time for different inertial force coefficients.

[Title Page](#)[Abstract](#)[Introduction](#)[Conclusions](#)[References](#)[Tables](#)[Figures](#)[|◀](#)[▶|](#)[◀](#)[▶](#)[Back](#)[Close](#)[Full Screen / Esc](#)[Printer-friendly Version](#)[Interactive Discussion](#)

**Forchheimer flow to a well considering time-dependent critical radius**

Q. Wang et al.

**Fig. 6.** Critical radius changes with time for different critical specific discharges.[Title Page](#)[Abstract](#)[Introduction](#)[Conclusions](#)[References](#)[Tables](#)[Figures](#)[|◀](#)[▶|](#)[◀](#)[▶](#)[Back](#)[Close](#)[Full Screen / Esc](#)[Printer-friendly Version](#)[Interactive Discussion](#)

## Forchheimer flow to a well considering time-dependent critical radius

Q. Wang et al.

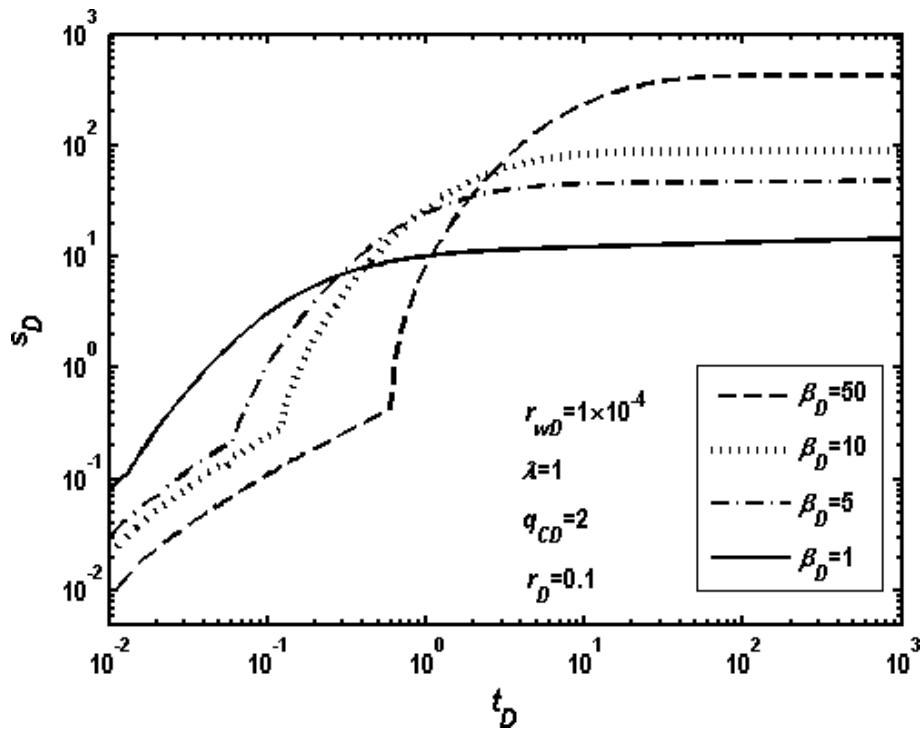


Fig. 7. Time-drawdown at  $r_D = 0.1$  for different inertial force coefficients in a log–log scale.

Title Page

Abstract

Introduction

Conclusions

References

Tables

Figures

◀

▶

◀

▶

Back

Close

Full Screen / Esc

Printer-friendly Version

Interactive Discussion



## Forchheimer flow to a well considering time-dependent critical radius

Q. Wang et al.

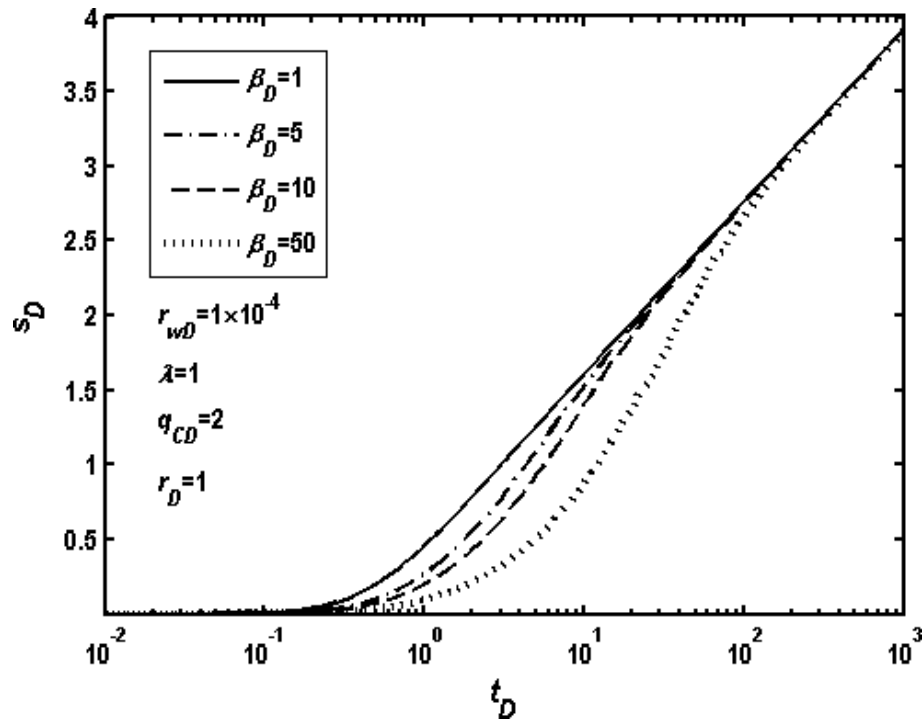


**Fig. 8.** Time-drawdown at  $r_D = 1$  for different inertial force coefficients in a semi-log scale.

Title Page

Abstract

Introduction

Conclusions

References

Tables

Figures

◀

▶

◀

▶

Back

Close

Full Screen / Esc

Printer-friendly Version

Interactive Discussion